声场声信息国家重点实验室年报

ANNUAL REPORT Volum 1

STATE KEY LABORATORY OF ACOUSTICS

第 1 卷　　1991

中国科学院声学研究所

声场声信息国家重点实验室年报

ANNUAL REPORT Volum 1

STATE KEY LABORATORY OF ACOUSTICS

第 1 卷 1991

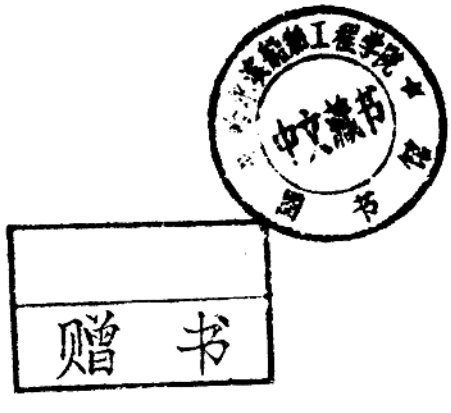

中国科学院声学研究所

前　言

声场声信息国家重点实验室自建成国家验收以来，正式工作已一年多了。一年来在各界的大力支持和实验室全体同志努力下，研究工作已逐步开展并取得了一些成果。一九九一年年报反映本实验室这一年所取得的成绩。

声波是人类感知外界信息，并进行信息交换和通信的主要手段。声波也是现代科学技术用于检测和遥感的重要手段。本实验室将声场和声信息结合起来，用现代信号处理技术进行研究，并提供所需的设备和手段，具有多通道联机实时处理能力。一年来，科学家们在本实验室中利用这些设备在水下声场模拟、海上实验数据处理、信号处理算法研究、语音信号处理、超声和空气声研究中取得了可喜的成绩。我深信今后本实验室在相关领域中会做出更多高水平的工作，为我国声学、语言、信号处理科学技术发展及相关高技术产业的建立和发展做出贡献。

本年报是本实验室的第一卷年报。我们已经有了一个良好的开端，希望今后能做出更大的成绩。

最后向热情支持与关怀本实验室工作的老一辈科学家汪德昭教授、马大猷教授和应崇福教授，向为本实验室的建立和发展做出贡献的各位同志以及为编辑出版本年报工作付出辛勤劳动的同志们表示感谢。

声场声信息国家重点实验室

学 术 委 员 会 主 任

侯自强

一九九一年十二月

声场声信息国家重点实验室简介

一、概　　况

声场声信息国家重点实验室是1987年国家计委批准筹建，1989年底建成，1990年2月通过国家验收，1990年9月批准正式对外开放。1991年3月召开了第一次学术会委员会会议，并进行了学术报告，讨论了实验室的研究方向，审定了"课题指南"，审批了1991年度的研究课题。

在实验室筹建过程中，实行边建设、边开放、边工作的方针，开展和支持了多项国家自然科学基金、"863"和"七五"攻关项目。至1990年底，实验室的固定与客座研究人员取得了多项具有国际先进水平的科研成果，其中"简正波声场变换与过滤的研究"、"脉冲超声在固体中散射的理论与实验研究"与"反转点会聚区理论与南海深海声道研究"分别获得国家自然科学二、三与四等奖，"浅海声传播损失数值预报"与"汉语语音特征研究"获中国科学院自然科学一等奖。在此期间，科研人员在国内外有影响的学术刊物上发表了论文116篇，培养了一批博士与硕士研究生，开展了国际交流与合作。

二、实验室的研究方向与主要研究内容

现代声学是和其它学科，电子学和信息科学相交叉而发展起来的。特别是现代数字信号处理技术和计算机技术的发展，赋予声学极大的新的生命力，使一个古老的声学学科变成一门现代化的生气勃勃的学科。声场声信息这个名称隐含声学与信息科学的交叉。声场与声信息的理论和应用是现代声学的重要标志.它的发展将对国防、海洋开发、工业发展、天然资源的探测、医学探测、环境保护、语言自动识别和合成有着重大意义。

研究声波与物质的相互作用，探索物质结构对声场规律的影响以及利用声波作为探测物质结构的方法是声学研究的基本内容。由于声波是人类传递信息的载体与获取信息的重要手段，声场与声信息理论和应用的密切结合成为现代声学的重要特点，而声信息的分析、处理和利用离不开现代信号处理理论和技术，因此，将声场物理与声信息的研究同信号处理理论和技术相结合是本实验室的重要特色，并以有关声探测与识别的理论和方法做为本实验室的研究重点。本实验室的主要研究方向如下:

1.声场理论以及物理与计算机模拟

通过现场实验以及物理与计算机模拟，研究声波在固体、液体和气体中的

传播规律以及声波与媒质间的相互作用，发展二维与三维非均匀媒质中声场传播、散射与吸收的理论和计算方法。

2.声场反演的理论与计算方法

声场反演理论是声探测与声成像的理论基础。重点研究海洋与大气媒质非均匀性的反演；海底分层结构及声学参数的提取；空气、液体与固体中目标物的逆散射与声成像理论和方法；声源与声散射体的探测与识别。

3.自然声源信息及其信号处理

通过接收处理发声物体的声信号所带信息是探测物体存在、确定其位置、判断其性质的基本方法。语音信号是人类传递与交流信息的重要手段，具有语言输入与输出能力是新一代人工智能计算机的重要特征，因此研究语言信号的分析、识别与合成具有特别重要的意义，语言信号处理是现代声学与信号处理研究中最活跃的分支之一。

4.声场时空处理的理论和技术

声探测与声遥感总是使用若干传感器从声场中接收信号，由于环境干扰背景的影响以及传输信道产生的信号畸变，会造成信号被淹没或使参数估计误差增大。信号处理的目的在于尽量消除干扰噪声以及信道畸变的影响，尽可能好地检测出有用信号并估计出其参数。声场最佳时空处理理论就是寻找最佳处理器的结构和它的性能极限，以便发挥各种信号处理器的潜力和提出改进方法。

根据上述研究方向，本实验室支持前沿新的学术思想，支持有宏大科学意义和应用前景的研究工作。主要研究内容有：

1.海洋声场及反演，浅海声场的简正波结构，简正波过滤的研究，波导中声定位研究。浅海声场起伏及声信号的时间空间相关特性，声信道时空变化的模式化，信道匹配的自适应理论，水声场的逆问题。弹性壳体的多辐射和声散射。

2.远距离水下声探测定位与识别：水声信号的分析，参数估计，识别。水声信号处理算法的研究。水声信号的实时及准实时处理及实现，舰船噪声识别，目标声反射信号的识别，水声信号识别专家系统、声图像处理。基阵的研究。

3.声信号处理：有关谱估计，正交变换和最佳滤波和自适应算法的研究。信号处理中的并行算法。波前阵列及脉动阵列处理机研究，信号处理的应用。高速信号处理的硬件实现。

4.空气声场的物理和计算机模拟：大气中声传播的理论和物理模拟研究。环境噪声场，交通噪声，飞机场噪声的物理和计算机模拟。利用计算机和信号处理技术控制空气中的声场，空气声场和振动的有源控制。有源消声的理论和

方法、利用计算机控制和改变室内声场的特性。

5.语言声学：语言产生的声学理论。语言信号分析。语言特征分析和提取、语言合成和文语转换。发音人适应的和任意发音人的语言识别。神经网络在语言识别中的应用。言语知觉特性和模型。汉语语音理解，语言自动翻译。

6.超声在不均匀介质中的传播和检测：超声在不均匀介质中的传播。超声成像，生物组织特征量的超声鉴别。超声在复合材料中的传播与检测。超声岩性测量。超声检测中的信号处理。声全息的理论和实验方法。

我们的目标是通过上述研究工作使本实验室成为我国发展声学科学与技术、培养声学科技人才的重要基地，成为开放国内外声学学术交流的一个重要场所，逐渐使本实验室在声场、声信息与信号处理研究方面跻身于国际先进行列。

三、对外开放的基本条件

实验室由信号处理中心和各分实验室组成，它们之间用计算机联网，各分实验室可以共享信号处理中心的硬、软件资源。分实验室有空气声场模拟实验室、超声实验室、语言声学实验室与水中声场模拟实验室。

信号处理中心配有 VAX 8350、VAX 750、VAX 3500、MicroII、VAX、Sun4／260 等计算机并用以太网连接，组成局部网络。各种记录、测量仪器、信号分析仪、谱分析仪与计算机接成一个整体。系统中配有阵处理机 AP500 作实时处理。并配有信号处理，有限元分析，数学分析等各种软件。

本实验室在水声、空气声、超声、信号处理与语言声学等方面有国内外著名的专家担任学术带头人。实验室具有良好的设备与工作条件，声学研究所提供了较好的后勤服务，可接纳客座研究人员 30 名，并具有很强的培养研究生的能力（研究生 15 名、博士生 4 名、博士后 2 名）。

声场声信息国家重点实验室

1991 年 12 月

一九九一年

声场声信息国家重点实验室年报

目　　录

Range and depth–averaged fields in ocean sound channels

Renhe Zhang and Wang Qin

(State Key Laboratory of Acoustics, Academia Sinica)

本文曾在 *J. Acoust. Soc. Am.*, 87(1990), No.2, 第 633 页上发表

Abstract By use of the generalized phase–integral approximation of the mode depth function and representing the square of the depth function as a sum of slow–varying and fast–varying components, a concise expression of the average intensity in an ocean channel is obtained by smooth averaging the intensities over range and depth. This expression is not divergent and will degenerate into the Brekhovskikh, Smith, and Weston one when the frequency approaches infinity. The caustic corrections in the vicinity of the source and its conjugate depths and the contributions of inhomogeneous waves are discussed and the numerical results for the linear, bilinear, and canonical channels are given.

INTRODUCTION

The field in an ocean sound channel usually involves a great number of rays or normal modes and has very complicated interference structure in space. Modern computers, in principle, may calculate the acoustic field in the ocean involving the interference structure, however, it is necessary to accurately know the acoustic parameters of the medium everywhere or a high price will be paid.For the long–range field, a small variation of the medium may cause a great change of relative phases among rays or modes. As a result, the fine structure of the field calculated is often inconsistent with observations. So, in many cases directly calculating the average field is of practical significance. Brekhovskikh, Smith, and Weston have deduced similar formulas of the average field (called the BSW formula)by using the ray method [1–3] the normal–mode method [4] and the acoustic flux method [5,6] repectively. Although the BSW formula has an advantage in concise form and clear physical meaning, it has some defects in that the BSW formual diverges at source and its conjugate depths and does not reveal the frequency dependence of field.

In this paper, proceeding from the normal–mode theory and taking the generalized phase–integral (GPI) approximation of the depth function, the range–and depth–averaged field is discussed. Section I recapitulates the GPI approximation of the depth function and its characteristics. SectionII discusses the intensity smooth averaged over range and depth for the receiver away from the source and its conjugate depths. and Sec. III deals with the caustic corrections in the vicinity of the source and its conjugate depths. Section IV

examines the contributions of inhomogeneous waves to the whole field. Section V gives some numerical resules and compares them with those from other methods.

I. GENERALIZED PHASE–INTEGRAL APPROXIMATION OF MODE DEPTH FUNCTION

When the frequency is higher than the critical frequency of the underwater sound channel, the field of harmonic point source is mainly determined by the waveguide modes; that is.

$$P=\sqrt{\frac{8\pi}{r}}\sum_{l=0}^{L}\psi_l(z_1)\psi_l(z_2)\sqrt{\nu_l}\exp(i\nu_l r+\frac{i\pi}{4}), \tag{1}$$

where z_1 and z_2 are the source and receiver depths, ν_l and $\psi_l(z)$are the eigenvalue and depth function of the waveguide mode, respectively.

The exact solution for the function $\psi_l(z)$ is hard to get. The depth function near and far away from the turning depths may be approximately expressed by using the Airy function and the WKB approximation, [7] resperctively. The GPI approximation with two parameters for the depth function of the waveguide mode in underwater sound channel was presented in Ref. [8]. Similarly, in this paper, the depth function $\psi_l(z)$is represented by using the following GPI approximation [9] with one parameter E:

$$\psi_l(z)=\sqrt{\frac{2}{S_l}}\begin{cases}\dfrac{\exp[-\int_z^{\eta_l}\sqrt{\nu_l^2-k^2(y)}\,dy]}{\sqrt{2}[Eb^{2/3}(z)+4\nu_l^2-4k^2(z)]^{1/4}}, & z<\eta_l,\\[2ex] \dfrac{\sin[\int_{\eta_l}^{z}\sqrt{k^2(y)-\nu_l^2}\,dy+\pi/4]}{[Eb^{2/3}(z)+k^2(z)-\nu_l^2]^{1/4}}, & \eta_l<z<\zeta_l,\\[2ex] \dfrac{(-1)^l\exp[-\int_{\zeta_l}^{z}\sqrt{\nu_l^2-k^2(y)}\,dy]}{\sqrt{2}[Eb^{2/3}(z)+4\nu_l^2-4k^2(z)]^{1/4}}, & \zeta_l<z,\end{cases} \tag{2}$$

where $k(z)=\omega/c(z)$, $E=0.875$, $b(z)=\left|dk^2(z)/dz\right|$, and S_l is the cycle distance of the mode, namely,

$$S_l=2\int_{\eta_l}^{\zeta_l}\frac{\nu_l dz}{\sqrt{k^2(z)-\nu_l^2}}. \tag{3}$$

Here η_l and ζ_l, respectively, are the turning depths above and below the channel axis and estimated from $k(\eta_l)=k(\zeta_l)=\nu_l$.As shown in Ref. [8], the GPI approximation (2)

degenerates into the WKB appoximation when z is far away from η_l and ζ_l, and approaches the Airy function in the vicinity of the turning depths η_l and ζ_l. In Fig.1, an example of the depth function is shown, where the solid line, circular points, and dashed line denote the exact solution, GIP, and WKB approximations, respectively.

The GIP approximation (2) not only has a simple from and sufficient accuracy for calculating the average field but it also has an important advantage that the square of $\psi_l(z)$ can be easily represented as a sum of the slow-varying component $\overline{\psi_l^2(z)}$ and the fast-varying component $\widetilde{\psi_l^2(z)}$, namely,

$$\psi_l^2(z) = \overline{\psi_l^2(z)} + \widetilde{\psi_l^2(z)}, \tag{4}$$

where

$$\overline{\psi_l^2(z)} = \begin{cases} \dfrac{\exp[-2\int_z^{\eta_l}\sqrt{v_l^2 - k^2(y)}\,dy]}{S_l[Eb^{2/3}(z) + 4v_l^2 - 4k^2(z)]^{1/2}}, \\ \qquad\qquad z < \eta_l, \\ \{S_l[Eb^{2/3}(z) + k^2(z) - v_l^2]^{1/2}\}^{-1}, \\ \qquad\qquad \eta_l < z < \zeta_l, \\ \dfrac{\exp[-2\int_{\zeta_l}^{z}\sqrt{v_l^2 - k^2(y)}\,dy]}{S_l[Eb^{2/3}(z) + 4v_l^2 - 4k^2(z)]^{1/2}}, \\ \qquad\qquad \zeta_l < z, \end{cases} \tag{5}$$

and

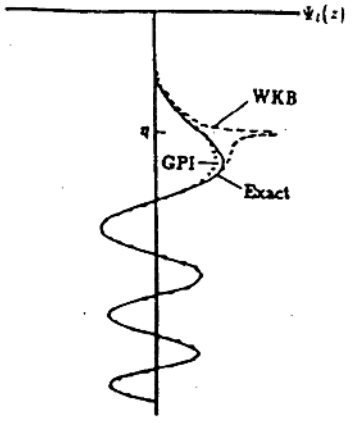

Fig.1 An example of the depth function

$$\widetilde{\psi_l^2(z)} = \begin{cases} \dfrac{\sin[2\int_{\eta_l}^{z}\sqrt{k^2(y)-\nu_l^2}\,dy]}{S_l[Eb^{2/3}(z)+k^2(z)-\nu_l^2]^{1/2}}, & \eta_l \leqslant z \leqslant \zeta_l, \\ 0, & \text{otherwise.} \end{cases} \tag{6}$$

The function $\overline{\psi_l^2(z)}$ corresponds to the "direct-current" component of $\psi_l^2(z)$ while $\widetilde{\psi_l^2(z)}$ corresponds to the "alternating-current" component. Figure 2 illustrates the diagrams of $\psi_l(z)$, $\psi_l^2(z)$,$\overline{\psi_l^2(z)}$,and $\widetilde{\psi_l^2(z)}$.

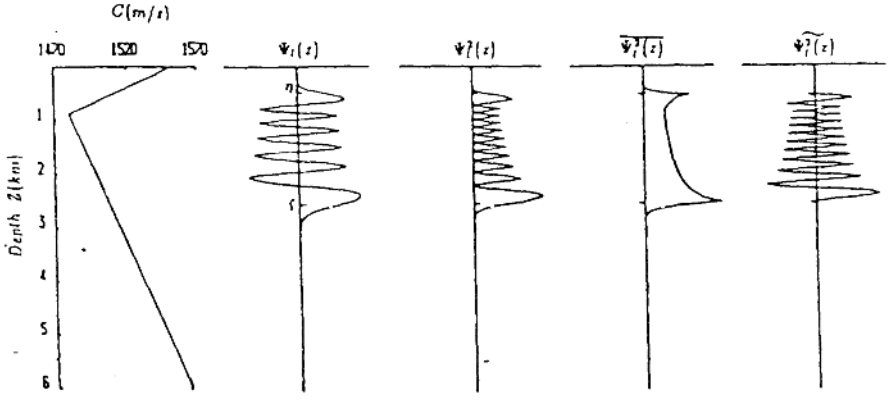

Fig. 2

Since the great majority of energy of a waveguide mode is concentrated on the range between its upper and lower turning depths, in most cases,it is permissible to take

$$\overline{\psi_l(z)} \approx \begin{cases} \{S_l[Eb^{2/3}(z)+k^2(z)-\nu_l^2]^{1/2}\}^{-1}, & \eta_l \leqslant z \leqslant \zeta_l, \\ 0, & \text{otherwise.} \end{cases} \tag{7}$$

II. INTENSITY SMOOTHLY AVERAGED OVER RANGE AND DEPTH

This section mainly discusses the average filed for the receiver away from the source and its conjugate depths. From Eq.(1), the sound intensity is obtained as

$$I(z_1,z_2,r) = \frac{8\pi}{r}\sum_l \psi_l^2(z_1)\psi_l^2(z_2)\nu_l + \frac{8\pi}{r}\sum_{l\neq m}\psi_l(z_1)\psi_l(z_2)\psi_m(z_1)\psi_m(z_2)\sqrt{\nu_l\nu_m}\exp[i(\nu_l-\nu_m)r], \tag{8}$$

where the first part varies with r slowly and smoothly and the second part, including all cross terms, oscillates with r rapidly.

Smooth-averaging over range and depth means that the operators $(1/\Delta r)\int_0^{\Delta r}\cdots dx$ and $(1/\Delta z)\int_0^{\Delta z}\cdots dy$ are applied to $I(z_1+y, z_2+y, r+x)$.

Note that $(v_l - v_{l+1}) \approx 2\pi/S_l$, if $\Delta r > S_l$, the cross terms in Eq.(8) can be omitted by smooth-averaging over range. Then, from Eq.(8), one obtains

$$\frac{1}{\Delta r}\int_0^{\Delta r} I(z_1, z_2, r+x)dx = \frac{8\pi}{r}\sum_l \psi_l^2(z_1)\psi_l^2(z_2)v_l. \tag{9}$$

By smooth-averaging over depth then, the intensity averaged over range and depth can be written as

$$I_{av}(z_1, z_2, r) = \frac{8\pi}{r}\sum_l \overline{\psi_l^2(z_1)\psi_l^2(z_2)}v_l \tag{10}$$

where

$$\overline{\psi_l^2(z_1)\psi_l^2(z_2)} = \frac{1}{\Delta z}\int_0^{\Delta z}\psi_l^2(z_1+y)\psi_l^2(z_2+y)dy. \tag{11}$$

It can be seen from Eq.(6) that the maximum oscillating period Z_l of fast-varying component is $\widetilde{\psi_l^2(z)}$ is located near the turning depth η_l and ζ_l is given by

$$Z_l \approx \frac{(3\pi/2)^{2/3}}{b^{1/3}(\eta_l)} \quad or \quad \frac{(3\pi/2)^{2/3}}{b^{1/3}(\zeta_l)} \tag{12}$$

When the sliding window Δz is greater than Z_l and the receiver is away from the source depth z_1 and its conjugate depth z_1^* (where the sound velocity is the same as that at the source), the fast-varying component $\widetilde{\psi_l^2(z)}$ can be omitted by smooth-averaging over depth, and then the following approximation may be taken:

$$\overline{\psi_l^2(z_1)\psi_l^2(z_2)} \approx \overline{\psi_l^2(z_1)}\ \overline{\psi_l^2(z_2)}, \tag{13}$$

where $\overline{\psi_l^2(z)}$is given by Eq.(5) or (7). Use $I_{SF}(z_1, z_2, r)$to denote the average intensity when the receiver is away from the source and its conjugate depths. Substituing Eqs. (13) and (7) into Eq. (10), one gets

$$I_{SF}(z_1, z_2, r) = \frac{8\pi}{r}\sum_l v_l/S_l^2[Eb^{2/3}(z_1) + k^2(z_1) - v_l^2]^{1/2} \times$$
$$\times [Eb^{2/3}(z_2) + k^2(z_2) - v_l^2]^{1/2}. \tag{14}$$

Since the terms of series (14) vary slowly with l, the summation can be approximate by the corresponding integration with respect to l. According to the relationship between the eigenvalue of a mode and the grazing angle of the corresponding eigenray, one has

$$v_l = k(h_0)\cos\alpha_0 = k(z_l)\cos\alpha_1 = k(z_2)\cos\alpha_2, \tag{15}$$

$$dl = S_l k(h_0) sin\alpha_0 d\alpha_0 / 2\pi \quad , \tag{16}$$

where α_0, α_1 and α_2 are the grazing angles at the channel axis h_0, source depth z_1, and receiver depth z_2,respectively, for the eigenray corrsponding to the l −th mode. By using Eqs. (15) and (16), the smooth−averaged intensity I_{SF} can be expressed as

$$I_{SF}(z_1,z_2,r) = (2C_1C_2 / rC_0^2)\int \frac{\sin(2\alpha_0)d\alpha_0}{S(\alpha_0)[D(z_1)+\sin^2\alpha_1]^{1/2}[D(z_2)+\sin^2\alpha_2]^{1/2}}, \tag{17}$$

where $c_0 = c(h_0)$, $c_1 = c(z_1)$,$c_2 = c(z_2)$, and

$$D(z) = E\left|\frac{1}{\pi f}\frac{dC(z)}{dz}\right|^{2/3} \tag{18}$$

Here, the integral variable α_0 is positive and the limits of integration in Eq. (17) are determined by the corresponding eigenrays. The formula (17) can also be generalized to the directional source as in Ref. [10].

Note that $D(z_1) = D(z_2) = 0$when the frequency is infinity. So_L, when $f=\infty$, the smooth−averaged intensity I_{SF} degenrates into the Brekhovskikh, Smith, and Weston formula of average field[1−6]:

$$I_{BSW} = \frac{2C_1C_2}{rC_0^2}\int \frac{\sin(2\alpha_0)d\alpha_0}{S(\alpha_0)sin\alpha_1 \sin\alpha_2}. \tag{19}$$

It is easy to show that the intensity I_{BSW} becomes infinity when $z_2 = z_1$ or $z_2 = z_1^*$ and is independent of the frequency.

III. CAUSTIC CORRECTIONS AT THE SOURCE AND ITS CONJUGATE DEPTHS

It is well understood that average field has large peaks at the source and at its conjugate depths due to caustics.[1, 5, 11, 12] Obviously, the peaks should not be infinity and their height and width should be dependent of the frequency and the velocity profile. This section discusses the average intensities in the vicinity of those depths.

When $z_2 \approx z_1$ or $z_2 \approx z_1^*$, Eq.(13) needs to be corrected. Near the sounce depth, let

$$\overline{\psi_1^2(z_1)\psi_1^2(z_1+\xi)} = F(\xi)\overline{\psi_1^2(z_1)}\ \overline{\psi_1^2(z_1+\xi)}, \tag{20}$$

where F(ξ)is the correction factor. Taking account of Eqs. (4)−(6)and(11), for $\eta_1 < z_1 < z_1 + \xi < \zeta_1$, one gets

$$F(\xi) \approx 1 + \frac{1}{2\Delta z}\int_0^{\Delta z} \cos(2\int_{z_1+z}^{z_1+z+\xi} \sqrt{k_2(y) - v_1^2}\, dy)dz. \tag{21}$$

When the receiver is located near the source depth, the modes for which theturning depths are close to the source depth [i.e, $\eta_1 \approx z_1$ and$\nu_l \approx k(z_1)$] make the main contributions to the field. For those modes near the source depth. the linear approximation $k^2(y) - \nu_1^2 \approx b(z_1)(y - z_1)$ may be taken. Then, from Eq(21). one yields

$$F(\xi) \approx 1 + \frac{1}{2\triangle z}\int_0^{\triangle z} \cos\left(\frac{4b^{1/2}(z_1)[(z+\xi)^{3/2} - z^{3/2}]}{3}\right)dz. \tag{22}$$

From Eq.(22),it is easy to get

$$F(0) = 3/2, \tag{23a}$$

$$F'(0) = 0, \tag{23b}$$

$$F''(0) = -b\triangle z. \tag{23c}$$

Obviously, the function F(ξ) dependent of the width $\triangle$z the sliding window. It may be reasonable to take $\triangle z = Z_l \approx (3\pi/2)^{2/3}/b^{1/3}(z_1)$. Thus Eq.(23c) becomes

$$F''(0) = -[3\pi b(z_1)/2]^{2/3}. \tag{24}$$

According to Eqs.(23a),(23b),and (24), the correction factor F(ξ) may be approximately expressed as

$$F(\xi) \approx 1 + \frac{1}{2}\exp(-\xi^2/\delta^2), \tag{25}$$

where

$$\delta = [2/3\pi b(z_1)]^{1/3} = [\,|\,3\pi a(z_1)k^2(z_1)\,|^{1/3}]^{-1} \tag{26}$$

Here, the quantity δ denotes the lobe width of F(ξ), and $\alpha(z_1)$ is the relative velocity gradient.Equation(26) shows that the higher frequency and the greater the velocity gradient, the narrower the lobe width. For example, if $\alpha(z_1) = 10^{-5}m^{-1}$ and $k(z_1) = 4m^{-1}$(near at the frequency of 1 kHz), one has $\delta = 8.7$m. By using Eq.(25),the average intensity in the vicinity of the source depth can be rewritten as

$$I_{av}(z_1, z_1 + \xi, r) \approx [1 + \frac{1}{2}\exp(-\xi^2/\delta^2)]I_{SF}(z_1, z_1 + \xi, r), \tag{27}$$

where I_{SF} is evaluated from Eq.(17). Equation (27) shows that

$$I_{av}(z_1, z_1 + \xi, r) \approx I_{SF}(z_1, z_1 + \xi, r)$$

except in a narrow range of the receiver depth near the source where

$$I_{av}(z_1, z_1, r) = \frac{3}{2}I_{SF}(z_1, z_1, r)$$

Calculation the average intensity in the vicinity of the source conjuate depth is rather

complicated. Here, only the average intensity exactly at the conjugate depth is given, that is,

$$I_{av}(z_1, z_1^*, r) = G(B) I_{SF}(z_1, z_1^*, r), \tag{28}$$

where

$$G(B) = 1 + \frac{1}{3(2\pi)^{2/3}} \int_0^{2\pi} \frac{\cos(B-1)\theta}{\theta^{1/3}} d\theta \tag{29}$$

and

$$B = \max\{[b(z_1) / b(z_1^*)]^{1/2}, [b(z_1^* / b(z_1)]^{1/2}\} \tag{30}$$

In Fig.3, the diagram of G(B) is shown where $G(1) = 3/2$ and $G(\infty) = 1$.

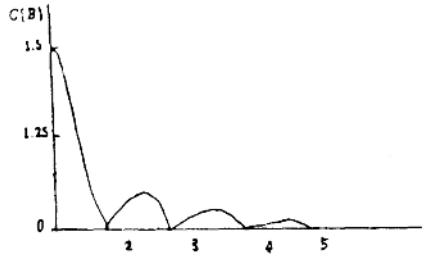

Fig. 3 Diagram of finction G(B)

IV. CONTRIBUTIONS OF INHOMOGENEOUS WAVES

Most theories of the average field did not take account of the contributions of inhomogeneous waves. In Eqs. (7),(14), and (17) mentioned above the inhomogeneous waves out of the upper and lower turning depths are neglected as well. In this section , the contributions of inhomogeneous waves to the whole field will be examined. For definiteness, assume that the source and receiver are above the channel axis, namely $z < z_2$. Taking account of the inhomogeneous waves, the expression (17) of the smoothaveraged intensity becomes

$$I_{total} = I_{SF} + \frac{2C_1C_2}{rC_0^2} \int_0^{\alpha_{1t}} \frac{\sin(2\alpha_0)\exp\{-\frac{4}{3}[-E\sin^2\alpha_2^2 / D(z_2)]^{3/2}\}}{S(\alpha_0)[D(z_1) + \sin^2\alpha_1]^{1/2}[D(z_2 - 4\sin^2\alpha_2]^{1/2}} d\alpha_0$$

$$+ \frac{2C_1C_2}{rC_0^2} \int \Big(\sin(2\alpha_0)\exp\{-\frac{4}{3}[-E\sin^2\alpha_1 / D(z_1)]^{3/2}$$

$$-\frac{4}{3}[-E\sin^2\alpha_2 / D(z_2)]^{3/2}\} / \Big\{S(\alpha_0)[D(z_1)$$

$$-4\sin^2\alpha_1]^{1/2}[D(z_2)-4\sin^2\alpha_2]^{1/2}\Big\}\Big)d\alpha_0 \tag{31}$$

where

$$\sin^2\alpha_1 = 1-[(c_1/c_0)\cos\alpha_0]^2, \qquad \sin^2\alpha_2 = 1-[c_2/c_0)\cos\alpha_0]^2. \tag{32}$$

The two integrals in the right side of Eq.(31) are the contributions of the inhomogeneous waves. The numerical result later shows that the contributions of inhomogeneous waves are very small.

V. NUMERICAL EXAMPLES

For the linear, bilinear, and canonical channels, the smooth-averaged intensities have been calculated by means of Eqs. (17), (27), and (28),and then the comparison of the results to those in Refs. [11] and [12] cab be made.

A. Linear channel

In Ref. [1], the average intensity is expressed as

$$I(z_1,z_2,r) = [1/r_0(z_1,z_2)](1/r), \tag{33}$$

where r_0 is called the transition distance. Reference [11] has directly calculated the incoherent summation of normal modes[correspond to the first part of the right side in Eq.(8)] and regarded it as the average intensity. Thus the transition distance r_0 at various source and receiver depths can be determined. For the linear profile of Fig.4 and the frequency of 100 Hz , 88 normal modes have been calculated. [11]

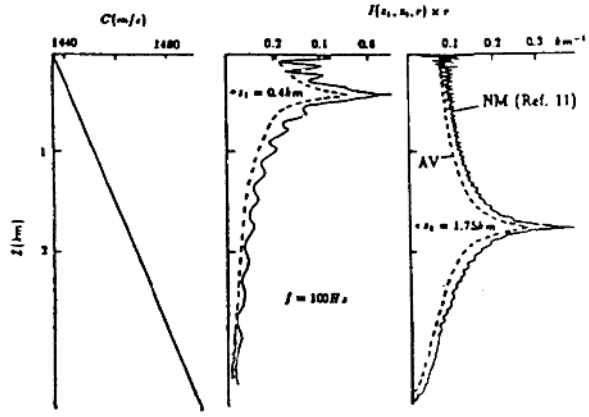

Fig. 4 Average intensities in a linear channel

Figure 4 shows the reciprocal $1/r_0$[*i.e.*$I(z_1,z_2,r)r$] versus the receiver depth for the source depths of 400 and 1750 m, respectively, where the solid lines denote the results from